Tuberculosis 129 (2021) 102100

Contents lists available at ScienceDirect

Tuberculosis

journal homepage: www.elsevier.com/locate/tube

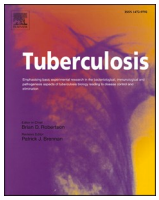

Reinvestigation of the structure-activity relationships of isoniazid

Pooja Hegde [a], Helena I.M. Boshoff [b], Yudi Rusman [c], Wassihun Wedajo Aragaw [d], Christine E. Salomon [c], Thomas Dick [d], Courtney C. Aldrich [a,*]

[a] Department of Medicinal Chemistry, University of Minnesota, Minneapolis, MN, 55455, USA
[b] Tuberculosis Research Section, Laboratory of Clinical Immunology and Microbiology, National Institute of Allergy and Infectious Disease, National Institutes of Health, Bethesda, MD, USA
[c] Center for Drug Design, University of Minnesota, Minneapolis, MN, 55455, USA
[d] Center for Discovery and Innovation, Hackensack Meridian Health, Nutley, NJ, 07110, USA

ARTICLE INFO

Keywords:
Isoniazid
SAR

ABSTRACT

Isoniazid (INH) remains a cornerstone for treatment of drug susceptible tuberculosis (TB), yet the quantitative structure-activity relationships for INH are not well documented in the literature. In this paper, we have evaluated a systematic series of INH analogs against contemporary *Mycobacterium tuberculosis* strains from different lineages and a few non-tuberculous mycobacteria (NTM). Deletion of the pyridyl nitrogen atom, isomerization of the pyridine nitrogen to other positions, replacement of the pyridine ring with isosteric heterocycles, and modification of the hydrazide moiety of INH abolishes antitubercular activity. Similarly, substitution of the pyridine ring at the 3-position is not tolerated while substitution at the 2-position is permitted with 2-methyl-INH **9** displaying antimycobacterial activity comparable to INH. To assess the specific activity of this series of INH analogs against mycobacteria, we assayed them against a panel of gram-positive and gram-negative bacteria, as well as a few fungi. As expected INH and its analogs display a narrow spectrum of activity and are inactive against all non-mycobacterial strains evaluated, except for **4**, which has modest inhibitory activity against *Cryptococcus neoformans*. Our findings provide an updated analysis of the structure-activity relationship of INH that we hope will serve as useful resource for the community.

1. Introduction

While Covid-19 has absorbed our attention and consumed a disproportionate fraction of infectious disease resources during the last year, the tuberculosis (TB) pandemic continues its silent onslaught with an estimated mortality in 2020 on the same level as Covid-19 [1,2]. TB is especially deadly for the millions of individuals, who are immunocompromised through co-infection with HIV or suffering with co-morbidities such as diabetes [3]. Despite substantial efforts over the last century, attempts to develop broadly effective vaccines against *Mycobacterium tuberculosis*, the principle etiological agent of TB, have been unsuccessful [4,5]. Several recent advances in the field have generated great enthusiasm that a durable and effective TB vaccine may be on the horizon. Small-molecule TB drugs will remain the principle means for addressing the TB pandemic for the foreseeable future.

Isoniazid (INH) first introduced into clinical practice in 1952, revolutionized the treatment of active and latent TB. In a review of one hundred of the most important drugs from the twentieth century, the American Chemical Society credited INH with potentially saving more lives than any other drug in human history [6]. INH remains a cornerstone of first-line combination therapy for its potent bactericidal activity during the initial phase of therapy [7]. INH is a prodrug bioactivated by the catalase-peroxidase KatG to generate an isonicotinoyl radical, which spontaneously reacts with nicotinamide adenine dinucleotide (NAD^+) (Fig. 1). The resulting NAD-INH adduct is a competitive nanomolar inhibitor of InhA, an enoyl acyl-carrier protein reductase that uses the cofactor NADH for biosynthesis of the mycolic acids that constitute up to 30% of the dry cellular weight of mycobacteria [8–11]. Depletion of mycolic acids in the mycobacterial cell envelope is bacteriostatic while the bactericidal mechanism has been correlated with a surge of ATP levels [12–14]. InhA consumes a large fraction of the cellular NADH pools to produce the saturated mycolic acids: inhibition of InhA likely redirects the NADH flux to respiration through the NADH:menaquinone oxidoreductases NDH-1 and NDH-2, which in turn stimulates ATP synthesis [13,15,16]. Dick and co-workers hypothesize the high level of ATP has pleiotropic effects on mycobacteria leading to the observed

* Corresponding author.
E-mail address: aldri015@umn.edu (C.C. Aldrich).

https://doi.org/10.1016/j.tube.2021.102100
Received 30 March 2021; Received in revised form 24 May 2021; Accepted 30 May 2021
Available online 5 June 2021

bactericidal activity since ATP is a central cofactor in metabolism [12]. Mycobacterial inhibitors of respiration including the recently approved bedaquiline (targets ATP synthase) and the investigational new drug telacebec (targets the respiratory bc_1 complex) predictably antagonize the activity of INH.

Consistent with its unique mechanism of action, isoniazid has a remarkable narrow spectrum of activity with a minimum inhibitory concentration (MIC) for susceptible *M. tuberculosis* isolates and members of the *M. tuberculosis* complex typically in the range of 0.03–0.1 μg/mL while gram-negative, gram-positive and most non-tuberculous mycobacteria (NTMs) are resistant with MICs greater than 64 μg/mL [17–22]. Structure-activity relationship (SAR) of INH revealed the hydrazide ($CONHNH_2$) moiety must be strictly maintained for activity while the pyridine heterocycle is optimal and replacement with other heterocycles results in sharp reductions in potency. Even conservative modifications such as introduction of a methyl group on the ring or isomerization of the nitrogen atom to the 2- or 3-positions obliterate activity [23,24]. However, much of the published data is qualitative in nature (+= active or - = inactive) [23–32] and most of the published quantitative *in vitro* activity of INH analogs is against *Mycobacterium bovis* BCG as a surrogate for *M. tuberculosis* [23,24]. When we attempted to compile all available data on currently approved antitubercular drugs [33], we faced difficulty due to the fragmentary and inconsistent nature of the published literature that is replete with circular citations of reviews and incomplete quantitative data against *M. tuberculosis*. Hence, we decided to reevaluate the SAR of isoniazid against a contemporary panel of mycobacterial strains including *M. tuberculosis* and NTM strains as well as some representative bacteria and fungi to provide a resource for the community.

2. Materials and methods

2.1. Chemistry

2.1.1. Methods and instrumentation

All glassware was dried in a 150 °C oven overnight. All chemicals, solvents, and glassware were purchased from either Fisher Scientific (Pittsburg, Pennsylvania), Ambeed (Chicago, Illinois) or Sigma Aldrich (St. Louis, Missouri). All reactions were performed under an inert atmosphere of argon. The chemical reactions were tracked using fluorescent silica gel-coated TLC plates and the separated components were visualized using UV light (254 nm) or staining with Ninhydrin. Compounds were purified by washing with hexanes and precipitating from dichloromethane and methanol (2:1). All final products synthesized or purchased, were characterized by ^{1}H NMR, ^{13}C NMR, IR and MS analyses. All new compounds were also characterized and confirmed by HRMS. Mass spectra were acquired either on an Agilent 1200/AB Sciex® API 5500 QTrap LC/MS/MS, using electrospray ionization or a single

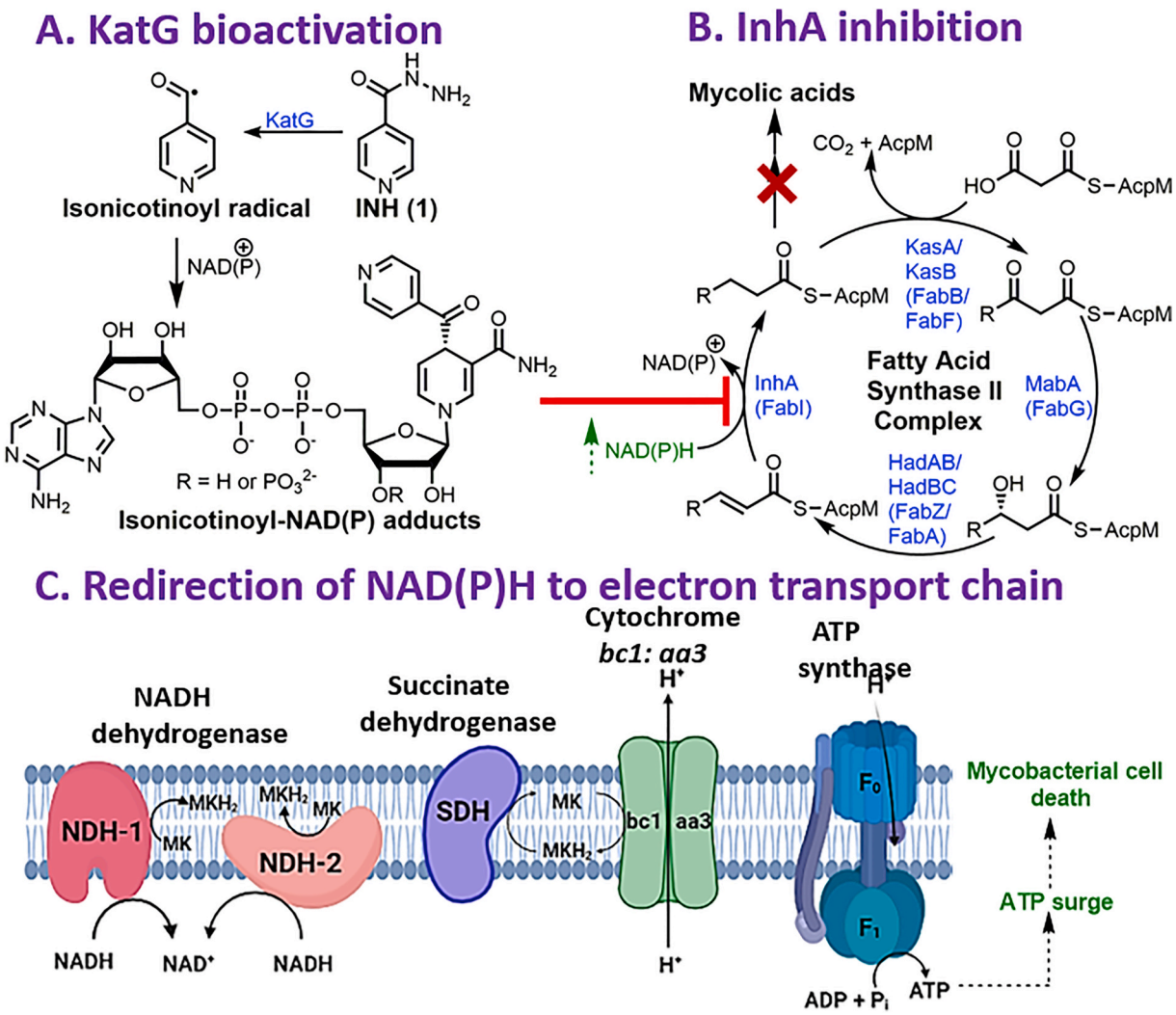

Fig. 1. Mechanism of action of INH **A.** Bioactivation of isoniazid to INH-NAD adduct. **B.** Inhibition of InhA in mycolic acid biosynthesis. **C.** NADH flux is redirected to respiration via electron transport chain resulting in increased ATP production.

quadrupole analyzer or on an Agilent 7200/Accurate-Mass Q-TOF GC/MS, using electron impact and a solid probe. All ^{1}H and ^{13}C NMR spectra were obtained on an Ascend™ 600 MHz Bruker spectrometer, and chemical shifts were reported relative to TMS. IR spectra were obtained on a Cary 30 FTIR diamond ATR Agilent FTIR spectrometer. Melting points were determined using a Thomas Hoover capillary melting point apparatus. All purchased and synthesized compounds were reported to have a purity of 95% and above, with the exception of **6**, which had a purity of 93%, tested by analytical high-performance liquid chromatography (HPLC), using a reversed phase C18 column (150 × 4.60 mm, Phenomenex, Torrance, United States) with the following gradient (all solvents contained 0.1% formic acid): from 95% water and 5% acetonitrile to 5% water and 95% acetonitrile over 18 min.

2.1.2. General synthetic method for synthesis of hydrazides from acids

The carboxylic acid (1 mmol) and triethylamine (TEA) (2 mmol) were mixed in dimethylformamide (DMF) (1 mL/mmol of acid) for 2 min (forming a sticky mass). Tetramethylfluoroformamidinium hexafluorophosphate (TFFH) (1 mmol) was then added to the mixture and the reaction stirred for 15 min at 23 °C whereupon the solution became clear. The mixture was cooled in an ice bath and hydrazine hydrate solution (2 mmol) was added. The reaction mixture was stirred at 4 °C for 20 min and then at 23 °C for another 45 min. The mixture was filtered using a Hirsch funnel and the solid was washed consecutively with hexanes, methylene chloride and methanol to afford the product, which was dried under high vacuum to constant weight and fully characterized.

2.1.3. General synthetic method for synthesis of hydrazides from methyl esters

The methyl ester (0.1 mmol, 1 equiv) was dissolved in methanol (7 mL) and hydrazine monohydrate (1 mmol, 10 equiv) was added. The reaction was stirred at 23 °C for 18 h, then the solvent and excess hydrazine were removed to afford the title compound, which was dried under high vacuum to constant weight and fully characterized.

2.1.4. Isonicotinic acid hydrazide (INH, 1)

The title compound was purchased from Ambeed. Melting point: 169 °C (reported [34,35] mp = 168–170 °C); R_f = 0.39 (95:5 CH_2Cl_2–MeOH); ^{1}H NMR (DMSO-d_6) δ 10.17 (s, 1H), 8.80–8.76 (m, 2H), 7.83–7.79 (m, 2H), 4.70 (s, 2H); ^{13}C NMR (DMSO-d_6) δ 164.4, 150.7, 140.7, 121.5 (^{1}H and ^{13}C NMR matched the reported values [35]); HRMS (EI) calcd for $C_6H_7N_3O$ $[M]^+$ 136.0631, found 136.0627 (error 2.9 ppm); IR (cm^{-1}) 1550, 1633, 1663, 2856, 3009, 3108, 3304.

2.1.5. Benzoic acid hydrazide (2)

The title compound was purchased from Ambeed. Melting point: 113 °C (reported [36] mp = 115 °C); R_f = 0.68 (95:5 CH_2Cl_2–MeOH); ^{1}H NMR (DMSO-d_6) δ 9.84 (s, 1H), 7.92–7.87 (m, 2H), 7.58 (t, J = 7.3 Hz, 1H), 7.52 (t, J = 7.5 Hz, 2H), 4.56 (s, 2H); ^{13}C NMR (DMSO-d_6) δ 166.4, 133.8, 131.5, 128.8, 127.4 (^{1}H and ^{13}C NMR matched the reported values [37]); HRMS (EI) calcd for $C_7H_8N_2O$ $[M]^+$ 136.0631, found 136.0635 (error 3.1 ppm); IR (cm^{-1}) 1554, 1607, 1661, 2874, 3014, 3198, 3301.

2.1.6. Pyridine-3-carboxylic acid hydrazide (3)

The title compound was purchased from Ambeed. Melting point: 164 °C (reported [38] mp = 161–162 °C); R_f = 0.43 (95:5 CH_2Cl_2–MeOH); ^{1}H NMR (DMSO-d_6) δ 9.96 (s, 1H), 8.97 (d, J = 2.2 Hz, 1H), 8.69 (dd, J = 4.8, 1.6 Hz, 1H), 8.16 (dt, J = 8.0, 2.0 Hz, 1H), 7.50 (dd, J = 8.0, 4.8 Hz, 1H), 4.57 (s, 2H); ^{13}C NMR (DMSO-d_6) δ 165.8, 151.3, 147.6, 135.5, 129.5, 123.8 (^{1}H and ^{13}C NMR matched the reported values [37]); HRMS (EI) calcd for $C_6H_7N_3O$ $[M]^+$ 137.0584, found 137.0589 (error 4.0 ppm); IR (cm^{-1}) 1541, 1641, 2866, 2942, 3005, 3324.

2.1.7. Pyridine-2-carboxylic acid hydrazide (4)

The title compound was prepared from pyridine-2-carboxylic acid and isolated as a white solid in 72% yield. Melting point: 101 °C; R_f = 0.86 (95:5 CH_2Cl_2–MeOH); ^{1}H NMR (DMSO-d_6) δ 10.69 (s, 1H), 8.78 (d, J = 4.7 Hz, 1H), 8.16–8.08 (m, 2H), 7.77–7.72 (m, 1H); ^{13}C NMR (DMSO-d_6) δ 163.5, 149.7, 149.1, 138.3, 127.5, 122.9; HRMS (EI) calcd for $C_6H_7N_3O$ $[M]^+$ 137.0584, found 137.0582 (error 0.9 ppm); IR (cm^{-1}) 1544, 1641, 1672, 3064, 3318.

2.1.8. Pyrimidine-4-carboxylic acid hydrazide (5)

The title compound was prepared from pyrimidine-4-carboxylic acid and isolated as an off-white solid in 69% yield. Melting point: 173 °C; R_f = 0.71 (95:5 CH_2Cl_2–MeOH); ^{1}H NMR (DMSO-d_6) δ 11.19 (s, 1H), 9.50 (d, J = 1.4 Hz, 1H), 9.22 (d, J = 5.0 Hz, 1H), 8.15 (dd, J = 5.0, 1.4 Hz, 1H); ^{13}C NMR (DMSO-d_6) δ 162.5, 159.2, 157.8, 155.8, 118.8; HRMS (EI) calcd for $C_5H_6N_4O$ $[M]^+$ 138.0536, found 138.0539 (error 2.4 ppm); IR (cm^{-1}) 1504, 1555, 1587, 1628, 1704, 2986, 3110, 3399, 3489.

2.1.9. Pyridazine-4-carboxylic acid hydrazide (6)

The title compound was prepared from pyridazine-4-carboxylic acid and isolated as a yellow solid in 71% yield. Melting point: 172 °C; R_f = 0.21 (95:5 CH_2Cl_2–MeOH); ^{1}H NMR (DMSO-d_6) δ 11.41 (s, 1H), 9.69 (s, 1H), 9.61 (d, J = 5.3 Hz, 1H), 8.19–8.15 (m, 1H); ^{13}C NMR (DMSO-d_6) δ 163.3, 152.9, 148.9, 130.0, 124.9 (^{1}H and ^{13}C NMR matched the reported values [37]); HRMS (EI) calcd for $C_5H_6N_4O$ $[M]^+$ 138.0536, found 138.0532 (error 3.0 ppm); IR (cm^{-1}) 1546, 1591, 1641, 1689, 2790, 3065, 3393.

2.1.10. Pyrazine-2-carboxylic acid hydrazide (7)

The title compound was purchased from Ambeed. Melting point: 171 °C; R_f = 0.58 (95:5 CH_2Cl_2–MeOH); ^{1}H NMR ($CDCl_3$) δ 9.31 (s, 1H), 8.71 (d, J = 2.4 Hz, 2H), 8.46 (t, J = 1.9 Hz, 1H), 4.03 (s, 2H); ^{13}C NMR ($CDCl_3$) δ 163.4, 147.7, 144.2, 143.7, 142.8 (^{1}H and ^{13}C NMR matched the reported values [37]); HRMS (EI) calcd for $[M]^+$ 138.0536, found 138.0532 (error 2.9 ppm); IR (cm^{-1}) 1513, 1577, 1644, 1674, 2817, 2906, 3218, 3305.

2.1.11. 3-Methylisonicotinic acid hydrazide (8)

The title compound was prepared from 3-methylisonicotinic acid and isolated as a light pink solid in 97% yield. Melting point: 124 °C; R_f = 0.45 (95:5 CH_2Cl_2–MeOH); ^{1}H NMR (CD_3OD) δ 8.46 (q, J = 0.8 Hz, 1H), 8.43–8.40 (m, 1H), 7.32 (d, J = 5.0 Hz, 1H), 2.38 (s, 3H); ^{13}C NMR (CD_3OD) δ 150.6, 146.5, 131.3, 121.4, 14.9; HRMS (EI) calcd for $C_7H_9N_3O$ $[M]^+$ 151.0740, found 151.0744 (error 2.86 ppm); IR (cm^{-1}) 1592, 1632, 1655, 3038, 3218, 3292.

2.1.12. 2-Methylisonicotinic acid hydrazide (9)

The title compound was prepared from 2-methylisonicotinic acid and isolated as a white solid in 96% yield. Melting point: 109 °C; R_f = 0.42 (95:5 CH_2Cl_2–MeOH); ^{1}H NMR ($CDCl_3$) δ 8.60 (dd, J = 5.4, 2.5 Hz, 1H), 7.82–7.79 (m, 1H), 7.48 (s, 1H), 7.36 (d, J = 5.1 Hz, 1H), 2.61 (s, 3H); ^{13}C NMR ($CDCl_3$) δ 167.0, 159.8, 150.0, 140.2, 120.5, 117.7, 24.4; HRMS (EI) calcd for $C_7H_9N_3O$ $[M]^+$ 151.0740, found 151.0738 (error 1.3 ppm); IR (cm^{-1}) 1536, 1610, 1654, 2859, 2927, 3056, 3165, 3274.

2.1.13. 3-Fluoroisonicotinoic acid hydrazide (10)

The title compound was prepared from 3-fluoroisonicotinic acid and isolated as a white solid in 73% yield. Melting point: 124 °C; R_f = 0.54 (95:5 CH_2Cl_2–MeOH); ^{1}H NMR (DMSO-d_6) δ 8.49 (1H, s), 8.41 (1H, d, J = 5.0 Hz), 7.58 (1H, t, J = 5.0 Hz); ^{13}C NMR (DMSO-d_6) δ 163.5, 156.6, 154.9, 145.7, 138.6, 128.8, 123.7; HRMS (EI) calcd for $C_6H_6FN_3O$ $[M]^+$ 155.0489, found 155.0483 (error 4.1 ppm); IR (cm^{-1}) 1544, 1562, 1620, 2129, 2590, 2916, 3053, 3212.

2.1.14. 2-Fluoroisonicotinoic acid hydrazide (11)

The title compound was prepared from 2-fluoroisonicotinic acid and isolated as a white solid in 72% yield. Melting point: 161 °C; $R_f = 0.71$ (95:5 CH_2Cl_2–MeOH); ^{1}H NMR (DMSO-d_6) δ 8.29 (dd, $J = 5.2$, 2.2 Hz, 1H), 7.74–7.64 (m, 1H), 7.45 (s, 1H); ^{13}C NMR (DMSO-d_6) δ 165.2, 149.6, 148.4 (d, $J = 15.0$ Hz), 120.0 (d, $J = 4.1$ Hz), 107.7, 107.3; HRMS (EI) calcd for $C_6H_6FN_3O$ $[M]^+$ 155.0489, found 155.0488 (error 1.0 ppm); IR (cm^{-1}) 1507, 1609, 1668, 2618, 2761, 3159, 3337.

2.1.15. Furan-2-carboxylic acid hydrazide (12)

The title compound was purchased from Ambeed. Melting point: 79 °C; $R_f = 0.59$ (95:5 CH_2Cl_2–MeOH); ^{1}H NMR ($CDCl_3$) δ 9.62 (s, 1H), 7.81 (d, $J = 1.7$ Hz, 1H), 7.08 (d, $J = 3.6$ Hz, 1H), 6.60 (dd, $J = 3.4$, 1.7 Hz, 1H), 4.42 (s, 2H); ^{13}C NMR ($CDCl_3$) δ 159.5, 146.6, 144.3, 114.9, 112.1; ^{1}H and ^{13}C NMR matched the reported values [37]; HRMS (EI) calcd for $C_5H_6N_2O_2$ $[M]^+$ 126.0424, found 126.0420 (error 3.3 ppm); IR (cm^{-1}) 1512, 1570, 1592, 1621, 1684, 3024, 3150, 3228, 3312.

2.1.16. 1H-Pyrrole-2-carboxylic acid hydrazide (13)

The title compound was prepared from methyl-1*H*-pyrrole-2-carboxylic acid and isolated as a white solid in 94% yield. Melting point: 227 °C; $R_f = 0.5$ (95:5 CH_2Cl_2–MeOH); ^{1}H NMR (DMSO-d_6) δ 11.48 (s, 1H), 9.28 (s, 1H), 6.89 (q, $J = 2.3$ Hz, 1H), 6.81–6.77 (m, 1H), 6.11 (q, $J = 2.7$ Hz, 1H), 4.39–4.36 (m, 2H); ^{13}C NMR (DMSO-d_6) δ 161.6, 125.4, 121.6, 109.9, 108.9; HRMS (EI) calcd for $C_5H_7N_3O$ $[M]^+$ 125.0584, found 125.0585 (error 0.9 ppm); IR (cm^{-1}): 1561, 1618, 2842, 2927, 3047, 3101, 3202, 3301.

2.1.17. Piperidine-4-carboxylic acid hydrazide (14)

The title compound was prepared through the Boc-deprotection of *N*-(tert-butyloxycarbonyl)piperidine-4-carboxylic acid hydrazide (**18**) (1 mmol) by stirring in 5 mL of (2:2:1) solution of TFA: THF: water at room temperature for 20 h. The reaction mixture was dried under vacuum and washed with hexanes and ethyl acetate forming a white solid precipitate in 85% yield. Melting point: 139 °C; $R_f = 0.61$ (95:5 CH_2Cl_2–MeOH); ^{1}H NMR (DMSO-d_6) δ 10.93 (s, 1H), 8.84 (d, $J = 191.4$ Hz, 2H), 3.31 (d, $J = 12.6$ Hz, 2H), 2.93 (d, $J = 14.0$ Hz, 2H), 2.59 (td, $J = 11.1$, 5.5 Hz, 1H), 1.88 (dd, $J = 14.1$, 3.7 Hz, 2H), 1.85–1.71 (m, 2H); ^{13}C NMR (DMSO-d_6) δ 173.0, 42.7, 37.3, 25.2; HRMS (EI) calcd for $C_6H_{13}N_3O$ $[M]^+$ 143.1053, found 143.1045 (error 5.4 ppm); IR (cm^{-1}) 1528, 1557, 1591, 1671, 1703, 2528, 2735, 2978, 3205.

2.1.18. N′-Isopropylisonicotinoic acid hydrazide (15)

The title compound was purchased from Ambeed. Melting point: 172 °C; $R_f = 0.58$ (95:5 CH_2Cl_2–MeOH); ^{1}H NMR ($CDCl_3$) δ 8.77–8.61 (m, 1H), 7.61–7.45 (m, 1H), 3.18 (hept, $J = 6.3$ Hz, 1H), 1.06 (d, $J = 6.3$ Hz, 3H); ^{13}C NMR ($CDCl_3$) δ 165.4, 150.7, 140.1, 120.7, 51.5, 20.8 (^{1}H and ^{13}C NMR matched the reported values [37]); HRMS (EI) calcd for $C_9H_{14}N_3O$ $[M + H]^+$ 180.1131, found 180.1132 (error 0.1 ppm); IR (cm^{-1}) 1544, 1596, 1640, 2877, 2933, 2971, 3235, 3302.

2.1.19. Pyridine-4-amide (16)

The title compound was purchased from Ambeed. Melting point: 156 °C; R_f = 0.54 (95:5 CH_2Cl_2–MeOH); ^{1}H NMR (DMSO-d_6) δ 8.74–8.70 (m, 2H), 8.25 (s, 1H), 7.79–7.75 (m, 2H), 7.73 (s, 1H); ^{13}C NMR (DMSO-d_6) δ 166.8, 150.7, 150.7, 141.8, 121.8 (^{1}H and ^{13}C NMR matched the reported values [37]); HRMS (EI) calcd for $C_6H_6N_2O$ $[M]^+$ 122.0475, found 122.0472 (error 2.0 ppm); IR (cm^{-1}) 1550, 1595, 1622, 1655, 2784, 3179, 3366.

2.1.20. Isonicotinic acid (17)

The title compound was purchased from Ambeed. Melting point >250 °C; $R_f = 0.34$ (95:5 CH_2Cl_2–MeOH); ^{1}H NMR (CD_3OD) δ 8.71–8.56 (m, 2H), 7.93–7.75 (m, 2H); ^{13}C NMR (CD_3OD) δ 166.2, 149.6, 139.4, 123.4 (^{1}H and ^{13}C NMR matched the reported values [37]); HRMS (EI) calcd for $C_6H_5NO_2$ $[M]^+$ 123.0315, found 123.0312 (error 2.2 ppm); IR (cm^{-1}) 1562, 1616, 1704.

2.1.21. N-(tert-butyloxycarbonyl)piperidine-4-carboxylic acid hydrazide (18)

The title compound was prepared from methyl *N*-(*tert*-butyloxycarbonyl)piperidine-4-carboxylate and isolated as a white solid in 87% yield; ^{1}H NMR ($CDCl_3$) δ 6.81 (d, $J = 9.5$ Hz, 1H), 4.08 (s, 2H), 3.82 (s, 2H), 2.67 (s, 2H), 2.15 (ddt, $J = 11.6$, 7.8, 3.9 Hz, 1H), 1.74–1.68 (m, 2H), 1.64–1.54 (m, 2H), 1.38 (s, 9H); ^{13}C NMR ($CDCl_3$) δ 175.2, 154.6, 79.7, 41.6, 28.4; HRMS (ESI) calcd for $C_{11}H_{21}N_3O_3$ $[M + Na]^+$ 266.1475, found 266.1481 (error 2.4 ppm); IR (cm^{-1}) 1525, 1629, 1682, 2847, 2933, 2982, 3321.

2.2. Pathogens and culture conditions for mycobacterial strains

M. abscessus bamboo [39] and *M. avium* 11 [40] were used as representative nontuberculous mycobacteria. *M. bovis* BCG Pasteur (ATCC 35734) and *M. tuberculosis* H37Rv (ATCC 27294) were obtained from the American Type Culture Collection. The other mycobacterial strains evaluated were *M. tuberculosis* Euro-American (CDC1551), *M. tuberculosis* Beijing (K03b00DS, K07b00DS, K12b00DS, NIH_G1DS, K04b00DS, K14b00DS, K09b00DS, HN878, K11b00DS, K05b00DS, 0K116), *M. tuberculosis* Uganda (NIH_G12), *M. tuberculosis* Haarlem (NIH_G11R), *M. tuberculosis* EAI (K5072429), *M. tuberculosis* West African 1 (NIH_G82, C02), *M. africanum*, *M. tuberculosis* Delhi, *M. bovis* (*AF2122*). These other strains were clinical isolates housed in the tuberculosis research section of the NIAID. Strains were grown in standard Middlebrook 7H9 broth (BD Difco) supplemented with 0.5% albumin, 0.2% glucose, 0.085% sodium chloride, 0.0003% catalase, 0.2% glycerol, and 0.05% Tween 80.

2.3. MIC determination for mycobacterial strains

The minimum inhibitory concentration (MIC) defined the concentration at which 90% inhibition of observable bacterial growth was determined by the microdilution method as previously described with modifications [39,41]. Briefly, 1 μL of a serial two-fold dilution of compounds in DMSO, were dispensed into flat bottom 96-well plates (Corning) using a D300e digital dispenser (Tecan). Test compounds were dissolved in 100% DMSO to 10 mM. To each well, 200 μL of a mid-log-phase bacterial culture ($OD_{600} = 0.05$) was dispensed to result in final concentration points ranging up to 100 μM. Culture plates were sealed using a Breathe-Easy sealing membrane (Fisher Scientific), put in a humidified airtight container, and incubated for 3 (*M. abscessus*), 4 (*M. avium*) or 5 (*M. bovis/M. tuberculosis*) days at 37 °C on an orbital shaker at 110 rpm. Turbidity/absorbance was read at 600 nm as a measure of growth inhibition using a Tecan TM Infinite 200 Pro microplate reader (Tecan). Percent growth was calculated relative to the cell density in the untreated wells and inhibition curves were plotted using Graph Pad Prism 9 software. The MIC, the concentration that reduces growth by 90% compared to untreated control, was deduced from the generated dose-response curves. Isoniazid and clarithromycin were used as controls. The other mycobacterial strains were grown in Middlebrook 7H9 medium supplemented with 0.5% BSA fraction V, 0.08% NaCl, 0.2% glucose, 0.2% glycerol and 0.05% Tween 80 (7H9/ADC/Tw) to an OD_{650nm} of 0.2. The culture was diluted 1000-fold in 7H9/ADC/Tw and 50 uL dispensed per well in round-bottom clear 96-well plate (Nunclon) containing 50 μL 7H9/ADC/Tw per well with or without 2-fold serial dilutions of compound. Plates were sealed in ziplock bags and incubated at 37 °C for 2 weeks. Growth was recorded after 1- and 2-weeks of growth by monitoring growth using an inverted enlarging mirror. The MIC was determined as the lowest concentration that completely inhibited growth. Positive control compounds included isoniazid and linezolid.

2.4. Pathogens and culture conditions for other pathogens

All compounds were tested against methicillin-resistant *Staphylococcus aureus* (MRSA) ATCC 43300, methicillin-sensitive *Staphylococcus aureus* (MSSA) IDRL-854, vancomycin-resistant *Enterococcus faecalis* (VRE) ATCC 51299, *Escherichia coli* ATCC 25922, *Acinetobacter baumannii* ATCC 19606, *Pseudomonas aeruginosa* ATCC 27853, *Klebsiella pneumoniae* ATCC 13883, *Cryptococcus neoformans* ATCC 66031 and *Candida albicans* ATCC 10231) using a modified broth dilution assay [42]. The strains of *S. aureus, E. coli* and *K. pneumoniae* were grown at 37 °C on Tryptic Soy media (TSA, TSB; BD Biosciences, San Jose, CA, USA). *A. baumannii* was cultured at 37 °C on nutrient medium (BD Biosciences, San Jose, CA, USA). Brain heart infusion (BHI; BD Biosciences, San Jose, CA, USA) was used for the cultivation of VRE at 37 °C. Yeast malt (YM; BD Biosciences, San Jose, CA, USA) media was used for cultivating *C. albicans* at 30 °C. *C. neoformans* was grown at 30 °C on Sabouraud dextrose medium.

2.5. MIC determination for gram-positive bacteria, gram-negative bacteria, and fungi

The test compounds were dissolved in DMSO at a stock concentration of 4 mM and kept at 4 °C for the bioassays. Bacteria or yeasts were grown to mid-log phase, diluted with fresh medium to an optical density at 600 nm (OD_{600}) of 0.030–0.060 and then diluted again 1:10. This suspension (195 μL) was added to wells in a 96 well microtiter plate (Sarstedt) and 5 μL of compound dissolved in DMSO was added to give a final concentration of 100–12.5 μM at 2.5% DMSO by volume. A DMSO negative control and standard antibiotic positive controls were included in each plate. Tetracycline (Sigma, St. Louis, MO, USA; 25 to 0.1 μg/mL in DMSO) was used as positive control against *S. aureus*, *B. subtilis*, *E. coli*, *P. aeruginosa*, *A. baumannii* and *K. pneumoniae.* Penicillin G (Sigma, St. Louis, MO, USA; 25 to 0.1 μg/mL) served as the positive control against VRE. Nystatin (Sigma, St. Louis, MO, USA; 25 to 0.1 μg/mL) was used as the positive control for *C. albicans* and *C. neoformans*. All compounds were tested in triplicate for each concentration. Plates were sealed with parafilm, placed in a Ziploc bag to prevent evaporation, and incubated at 30 °C (fungi) or 37 °C (bacteria) for 16–20 h (48 h for *C. neoformans*). The OD_{600} values for each well were determined with a plate reader (Biotek, EL800) and the data were standardized to the DMSO control wells after subtracting the background from the blank media wells.

3. Results

3.1. Chemistry

A systematic series of 16 analogs (Fig. 2, panel A) was prepared to explore the structure-activity relationships and importance of each atom of isoniazid. The hydrazide derivatives were either purchased or synthesized by condensing aromatic acids with anhydrous hydrazine in the presence of tetramethylfluoroformamidinium hexafluorophosphate (TFFH) as a coupling agent that generates acylfluorides from the corresponding carboxylic acids (Fig. 2, panel B) [43]. Along with TFFH, other conventional peptide coupling agents including HOBt-EDC, DCC-DMAP, PyBOP and HBTU were evaluated for the synthesis of these compounds, but we observed better conversions with TFFH and higher isolated yields. Purification of INH analogs using TFFA was straightforward and pure compounds were readily isolated through recrystallization from dichloromethane and methanol (2:1). Compounds **4**–**6** and **8**–**11** were synthesized using TFFH coupling with yields ranging from 69 to 97%. Alternatively, two of the analogs, **13**–**14** were synthesized by a substitution reaction of the methyl ester with hydrazine monohydrate (Fig. 2, panel C) [44]. The identity of the purchased and synthesized compounds was confirmed by measurement of the proton and carbon NMR, IR and melting points while the purity was determined by HPLC.

3.2. Mycobacterial activity

M.tuberculosis forms six main lineages and 15 sub-lineages, which are associated with different geographical locations [45,46]. The INH analogs were assayed for their activity against *M. tuberculosis* from 5 of the 6 different lineages, based on their availability during testing. The observed activity did not significantly vary across the lineages tested (Table 1). To assess the importance of the pyridine ring of INH (**1**), we evaluated the benzene analog **2**. As expected, deletion of the nitrogen

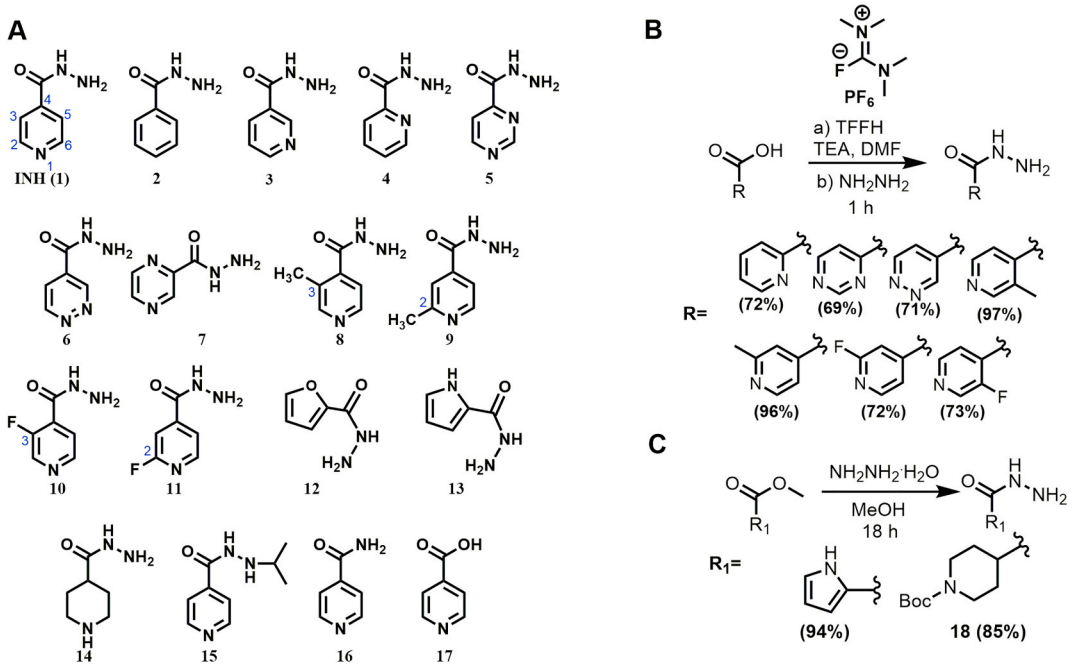

Fig. 2. Isoniazid analogs and synthetic schemes. A. Isoniazid analogs studied in this paper, **B.** General synthetic method for synthesis of hydrazides from acids, **C.** General synthetic method for synthesis of hydrazides from methyl esters.

Table 1
MIC values for active INH analogs against *M. tuberculosis* from different lineages.

Mycobacterium tuberculosis lineages	Lineage number	MIC_{90} (μM)[a]						
		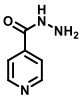	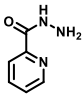	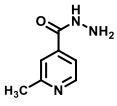	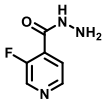	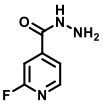	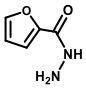	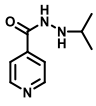
		INH	4	9	10	11	12	15
Drug susceptible: East Asian (10)	2	0.2–0.4	12.5–100	0.2–0.3	50–74	50–74	7.8 (1)	74–100
Drug susceptible: Euro-American (1)	4	0.2	20–50	0.2	50–74	50–74	>100	100
Drug susceptible: West African 2 (1)	6	0.4	12.5	0.2	50	50	>100	100
Drug susceptible: East African-Indian (1)	1	0.4	20	0.4	50	50	1.56	50
Drug resistant: West African 1 (2)	5	0.2	12.5–25	0.2–0.4	50–100	50–100	>100	50–100
Extremely Drug Resistant: East Asian (1)	5	12.5	25	25	>100	74	>100	>100

[a] MIC_{90} was determined using a microbroth dilution assay in Middlebrook 7H9/ADC/Tween medium with a DMSO negative control and standard isoniazid positive controls included in each plate. Number of strains tested are represented in parenthesis. Drug susceptible strains were susceptible to all anti-TB agents, drug resistant strains were resistant to moxifloxacin and cycloserine, while the extremely drug resistant strains were resistant to isoniazid, fluoroquinolones, rifamycins, ethambutol, streptomycin, cycloserine and prothionamide. Compounds not included in the table showed MIC values greater than 100 μM for all lineages and strains of *M. tuberculosis* tested.

atom completely abolished all activity (MIC > 100 μM). Similarly, transposition of the nitrogen atom to the adjacent positions with 3-pyridyl analog **3** obliterated activity against all *M. tuberculosis* strains. Interestingly, the 2-pyridyl analog **4** retained some activity with MICs ranging from 12.5 to 100 μM against the 16 strains evaluated. Incorporation of an additional nitrogen in the pyridine ring of INH with pyrimidine, pyridazine and pyrazine bioisosteres in **5**–**7** also abolished mycobacterial activity. Next, substitutions on the pyridine ring of INH with methyl and fluorine at the 2 and 3 positions was studied. The 2-methyl substituted analog **9** was equipotent to INH while 2-fluoro **11** displayed an astonishing 300-fold loss in potency indicating limited flexibility at the 2-position. Neither of the 3-substituted analogs **8** or **10** were active at 100 μM, demonstrating substitution at the 3-position is not tolerated. We also explored some non-conservative replacements of the pyridine ring with furan, pyrrole and piperazine analogs **12**–**14**. The furan **12** was inactive against most lineages of *M. tuberculosis*, with the exception of drug susceptible strains of the East African Indian origin, against which it had an MIC of 1.56 μM, whereas the pyrrole **13** and piperidine **14** analogs were inactive against most lineages of *M. tuberculosis* at the highest concentration tested (MIC >100 μM). Functional group replacement of the hydrazide group of INH with an amide **l6** or carboxylic acid **17** also obliterated activity confirming the importance of the hydrazide pharmacophore. Lastly, substitution of the N-2 atom of the hydrazide with an isopropyl group in **15** was poorly tolerated resulting in a weakly active compound. Pyridine-2-carboxylic acid hydrazide **4**, 2-methyl INH **9**, 3-fluoro INH **10**, 2-fluoro INH **11**, furan-2-carboxylic acid hydrazide **12** and N-isopropyl INH **15** were moderately active against drug susceptible and drug-resistant *M. tuberculosis* from different lineages, but were poorly active against an extremely drug-resistant *M. tuberculosis* strain.

The active compounds were further tested against various mycobacterial species including *M. bovis* (BCG) and non-tuberculous mycobacteria (NTM) including *M. abscessus* and *M. avium*. These NTMs were chosen since they are an increasing health concern globally due to their inherent resistance to a variety of drugs used for the treatment of TB [47]. All of the analogs were inactive at the maximum concentration tested (100 μM) with an exception of 2-methyl analog **9**, which showed modest activity against *M. avium* with an MIC of 12.5 μM (Table 2).

Compounds **1**–**17** were also evaluated against a panel of gram-positive and gram-negative bacteria to assess their antibacterial spectrum of activity. The panel of gram-positive bacteria included *Bacillus subtilis*, methicillin resistant (M.R) and susceptible (M.S) strains of *Staphylococcus aureus*, vancomycin resistant *Enterococcus faecalis* while the panel of gram-negative bacteria consisted of *Escherichia coli, Klebsiella pneumoniae, Pseudomonas aeruginosa* and *Acinetobacter baumannii*.

Table 2
MIC values for INH analogs active against BCG and NTMs.

Pathogen	MIC_{90} (μM)[a]	
	INH	9
Mycobacterium tuberculosis (H37Rv)	0.8	1.6
Mycobacterium bovis (BCG)	0.8	1.6
Mycobacterium avium	6.25	12.5
Mycobacterium abscessus	>100	>100

[a] MIC_{90} was determined using a microbroth dilution assay with a DMSO negative control and standard isoniazid positive controls included in each plate. All compounds were tested in triplicate for each concentration Compounds not included in the table showed MIC values greater than 100 μM for all strains of mycobacteria tested.

The compounds were also screened against the fungal strains *Candida albicans* and *Cryptococcus neoformans*. INH and most of the analogs were inactive with no inhibition of growth observed, even at the maximal concentration of drug tested (100 μM). However, 2-pyridyl analog **4**, showed weak, but reproducible antibacterial activity against gram-positive bacteria with an MIC of 100 μM against methicillin-sensitive *Staphylococcus aureus,* as well as some antifungal activity against *Cryptococcus neoformans* and *Candida albicans* with an MIC of 25 μM and 100 μM, respectively (Table 3).

4. Discussion

The goal of this study was to evaluate the antibacterial activity of INH and its structural analogs against contemporary gram-positive bacterial, gram-negative bacterial, fungal and mycobacterial strains. Our data generally aligns with previously described results. We confirm that INH is optimal for antimycobacterial activity and reconfirm the essentiality of the pyridine nitrogen and the hydrazide moiety for the activity of INH. Any major structural modification made to INH resulted in a significant loss of potency. 2-Fluoro INH **11**, 2-furan carboxylic acid hydrazide **12** and *N*-isopropyl INH **15** were reported to possess potent antimycobacterial properties with MICs of 2.5, 0.5 and 2.2 μM, respectively, against *M. tuberculosis* var. *Bovis* [24,25,27]. However, we observed these analogs are weakly active with MICs of over 50 μM against most of the *M. tuberculosis* clades tested. Notably, *N*-isopropyl INH **15** also known as iproniazid was initially used to treat TB and later shown to possess antidepressant activity through inhibition of monoamine oxidase, but was ultimately withdrawn from the market due to hepatoxicity [48,49]. The *in vivo* activity of **15** is likely caused by

Table 3
MIC values of **4** against other pathogens.

Pathogen	MIC_{90} (μM)[a]	
	INH	4
Bacillus subtilis	>100	>100
Staphylococcus aureus, MRSA	>100	>100
Staphylococcus aureus, MSSA	>100	100
vancomycin-resistant *Enterococcus faecalis*	>100	>100
Klebsiella pneumoniae	>100	>100
Pseudomonas aeruginosa	>100	>100
Acinetobacter baumannii	>100	>100
Escherichia coli	>100	>100
Candida albicans	>100	100
Cryptococcus neoformans	>100	25

[a] MIC_{90} was determined using a microbroth dilution assay with a DMSO negative control and standard antibiotic positive controls included in each plate. Tetracycline was used as positive control against *S. aureus*, *B. subtilis*, *E. coli*, *P. aeruginosa*, *A. baumannii* and *K. pneumoniae*. Penicillin G served as the positive control against VRE. Nystatin was used as the positive control for *C. albicans* and *C. neoformans*. All compounds were tested in triplicate for each concentration. Compounds not included in the table showed MIC values greater than 100 μM against all pathogens tested.

metabolism through *N*-dealkylation to release isoniazid [48,49].

On the other hand, we observed 2-methyl INH **9** was equipotent to INH with an MIC of 1.6 μM. We found a single study upon further literature review from 1976 that reported an MIC of 5 μM for **9** against a *M. tuberculosis* H37Rv strain that was 5-fold higher than INH in the same study [50,51]. Interestingly, the 2-fluoro analog **11** is weakly active, indicating limited flexibility at the 2-position. Lastly, pyridine-2-carboxylic acid hydrazide **4** and 3-fluoro INH **10,** which have not been previously described, showed weak anti-TB activity.

INH and its analogs selectively inhibit *M. tuberculosis* and are poorly active against other NTMs. Nevertheless, we observed 2-methyl INH **9** is active against *M. avium*. We also evaluated the activity of the entire suite of analogs against a panel of gram-positive and gram-negative bacteria and reconfirmed their narrow spectrum of activity and high selectivity towards mycobacteria. Interestingly, 2-pyridyl **4** possesses modest antifungal activity against *Cryptococcus neoformans*.

INH is a prodrug and its activity depends on two factors: bioactivation by KatG to form an isonicotinoyl-NAD (INH-NAD) adduct and subsequent inhibition of InhA by the INH-NAD adduct. Bioactivation by KatG is further divided into an initial binding/oxidation reaction to an acyl radical followed by the 'spontaneous' formation of the INH-NAD adduct [52–54]. Magliozzo demonstrated that five close INH analogs **2**–**4** and **12** and **13** all bound KatG more tightly than INH as measured by stopped-flow spectrophotometry and isothermal calorimetry (Table 4) [54,55]. While it was more difficult to quantify, all of the aforementioned analogs appeared to be efficiently oxidized to acyl radical species as measured indirectly by reduction of heme cofactor within the active site of KatG [54,55]. However, only INH and pyridine-2-carboxylic acid hydrazide **4** were shown to form an acyl-NAD adduct *in vitro* when co-incubated with NAD^+. INH analogs with substitutions on the pyridine ring were not studied by Magliozzo; however, we predict the 2-methyl INH **9** would also form an acyl-NAD adduct. The differing reactivity of the acyl radicals with NAD^+ may be due to differential stability/reactivity of the acyl radical species or alternatively suggests the second step may also be catalyzed by InhA. In support of this latter hypothesis, Loewen and co-workers were able to successfully co-crystallize InhA with INH and NAD^+ bound near the active site of a KatG homolog from *Burkholderia pseudomallei* [56]. The initial oxidation of acyl-hydrazides by KatG appears to be fairly promiscuous, but the subsequent reaction with NAD^+ is restrictive and thus controls the substrate specificity of prodrug activation. The seminal study by Tonge co-workers showed the INH-NAD adduct is slow-tight-binding inhibitor of InhA with a K_i of 0.75 nM; however, this study also revealed benzoyl-NAD was an equally potent inhibitor suggesting InhA may have broader substrate specificity [55]. Indeed, pyridomycin or nature's isoniazid, is a natural product that also inhibits InhA and whose binding closely overlaps with the INH-NAD adduct [57]. The observed SAR of INH thus appears to largely reflect the restricted substrate specificity for acyl-NAD adduct formation rather than the initial KatG oxidation and subsequent InhA inhibition.

Table 4
Binding affinities for KatG, ability to undergo oxidation and activation to an acyl-NAD adduct, and inhibition constants of the corresponding acyl-NAD adduct towards InhA.

Compound	K_d (μM) for KatG	Forms acyl-NAD adduct	K_i (nM) of acyl-NAD adduct for InhA
1 (INH)	41.7	Yes	0.75
2 (Benzoic acid hydrazide)	2.1	No	<1
3 (Pyridine-3-carboxylic acid hydrazide)	4.5	No	–
4 (Pyridine-2-carboxylic acid hydrazide)	1.4	Yes	–
12 (Furan-2-carboxylic acid hydrazide)	1.4	No	–
13 (1H-Pyrrole-2-carboxylic acid hydrazide)	5.2	No	–

In conclusion, we confirm the tight structure-activity relationships of INH and its narrow spectrum of activity. We found some minor inconsistencies with previous reported literature and surprisingly discovered that *N*-isopropyl INH **15** is inactive against *M. tuberculosis in vitro*, despite having reported *in vivo* activity [24,32,48,49], a result that can be reconciled if **15** is metabolized to INH *in vivo*. We also discovered 2-methyl INH **9** is equipotent to INH, which to the best of our knowledge is the first report of any INH analog with equivalent activity. Isoniazid continues to reign supreme as the optimal compound, but small substituents at the 2-position of the pyridine, such methyl found in **9** or other small groups such as fluoromethyl and difluoromethyl could potentially offer incremental advances over INH if they display reduced toxicity and/or an improved pharmacokinetic profile.

Credit author contribution statement

Pooja Hegde: Conceptualization, Data curation, Investigation, Project administration, Validation, Visualization, Writing-original draft, reviewing and editing; **Helena I. M. Boshoff:** Data curation, Formal analysis, Resources, Writing-reviewing, and editing; **Yudi Rusman**: Data curation, Formal analysis, Validation; **Wassihun Wedajo Aragaw**: Data curation, Formal analysis, Validation; **Christine E. Salomon**: Resources, Supervision, Writing-reviewing, and editing; **Thomas Dick**: Resources, Supervision, Writing-reviewing, and editing; **Courtney C. Aldrich**: Conceptualization, Supervision, Resources, Funding acquisition, Writing-reviewing, and editing

Acknowledgments

This work was supported by grants (AI136445 and AI143784) from the National Institutes of Health and in part by the Intramural Research Program of NIAID (AI000693). The NMR facility used for the characterization of compounds was supported in part by a NIH S10 instrumentation grant OD021536 (G. Veglia).

References

[1] World Health Organization. Tuberculosis and COVID-19 [cited 2021 21st March]; Available from: https://www.who.int/teams/global-tuberculosis-programme/covid-19; 2020.
[2] Centers for disease Control and Prevention. Treating TB during the time of COVID-19. 18th August, 2020 [cited 2021 21st March]; Available from: https://www.cdc.gov/globalhealth/stories/2020/tb-covid.html; 2020.

[3] World Health Organization. Global tuberculosis report [cited 2021 21st March]; Available from: https://apps.who.int/iris/bitstream/handle/10665/336069/9789240013131-eng.pdf; 2020.
[4] Moliva JI, Turner J, Torrelles JB. Immune responses to Bacillus calmette-guérin vaccination: why do they fail to protect against *Mycobacterium tuberculosis*? Front Immunol 2017;8. 407-407.
[5] Sable SB, Posey JE, Scriba TJ. Tuberculosis vaccine development: progress in clinical evaluation. Clin Microbiol Rev 2019;33(1):e00100–19.
[6] Wang L. Isoniazid. In: Chemical & Engineering News Archive. 83. ACS; 2005. p. 76. https://doi.org/10.1021/cen-v083n025.p076.
[7] World Health Organization-Stop Tb Initiative. Treatment of tuberculosis: guidelines. Geneva, Switzerland: World Health Organization; 2010. p. 147.
[8] Ottenhoff TH, et al. Control of human host immunity to mycobacteria. Tuberculosis 2005;85(1–2):53–64.
[9] Vilcheze C, Jacobs Jr WR. The mechanism of isoniazid killing: clarity through the scope of genetics. Annu Rev Microbiol 2007;61:35–50.
[10] Srivastava S, Ernst JD. Cell-to-cell transfer of *M. tuberculosis* antigens optimizes CD4 T cell priming. Cell Host Microbe 2014;15(6):741–52.
[11] Timmins GS, Deretic V. Mechanisms of action of isoniazid. Mol Microbiol 2006;62(5):1220–7.
[12] Shetty A, Dick T. Mycobacterial cell wall synthesis inhibitors cause lethal ATP burst. Front Microbiol 2018;9. 1898-1898.
[13] Zeng S, et al. Isoniazid bactericidal activity involves electron transport chain perturbation. Antimicrob Agents Chemother 2019;63.
[14] Lee BS, et al. Inhibitors of energy metabolism interfere with antibiotic-induced death in mycobacteria. J Biol Chem 2019;294(6):1936–43.
[15] Vilcheze C, et al. Altered NADH/NAD+ ratio mediates coresistance to isoniazid and ethionamide in mycobacteria. AAC (Antimicrob Agents Chemother) 2005;49(2):708–20.
[16] North EJ, Jackson M, Lee RE. New approaches to target the mycolic acid biosynthesis pathway for the development of tuberculosis therapeutics. Curr Pharmaceut Des 2014;20(27):4357–78.
[17] Ghodousi A, et al. Isoniazid resistance in *Mycobacterium tuberculosis* is a heterogeneous phenotype composed of overlapping MIC distributions with different underlying resistance mechanisms. Antimicrob Agents Chemother 2019;63(7). e00092-19.
[18] Burke RM, Coronel J, Moore D. Minimum inhibitory concentration distributions for first- and second-line antimicrobials against *Mycobacterium tuberculosis*. J Med Microbiol 2017;66(7):1023–6.
[19] Schon T, et al. Evaluation of wild-type MIC distributions as a tool for determination of clinical breakpoints for *Mycobacterium tuberculosis*. J Antimicrob Chemother 2009;64(4):786–93.
[20] Li G, et al. Antimicrobial susceptibility of standard strains of nontuberculous mycobacteria by microplate Alamar Blue assay. PloS One 2013;8(12):e84065.
[21] Maurer FP, et al. Differential drug susceptibility patterns of Mycobacterium chimaera and other members of the *Mycobacterium avium*-intracellulare complex. Clin Microbiol Infect 2019;25(3):379 e1–7.
[22] DeStefano MS, Shoen CM, Cynamon MH. Therapy for *Mycobacterium kansasii* infection: beyond 2018. Front Microbiol 2018;9:2271.
[23] Fox HH, Gibas JT. Synthetic tuberculostats. VIII. Acyl derivatives of isonicotinyl hydrazine. J Org Chem 1952;18:1375–9.
[24] Bernstein J, et al. Chemotherapy of tuberculosis. VI. Derivatives of isoniazid. J Org Chem 1952;65:354–65.
[25] Bernstein J, et al. Chemotherapy of experimental tuberculosis. V. Isonicotinic acid hydrazide (Nydrazid) and related compounds. Am Rev Tubercul 1952;65:357–64.
[26] Fox HH. The chemical attack on tuberculosis. Trans N Y Acad Sci 1953;15:234–42.
[27] Bernstein J, et al. Chemotherapy of experimental tuberculosis. VIII. Heterocyclic acid hydrazides and derivatives. Am Rev Tubercul 1952;65:366–75.
[28] Kakimoto S, Tone I. Antituberculous compounds. 23. Alkyl- and acylisonicotinic acid hydrazides. J Med Chem 1965;8(6):868.
[29] Fox HH. Synthetic tuberculostats. III. Isonicotinaldehyde thiosemicarbazone and some related compounds. J Org Chem 1952;17:555–62.
[30] Fox HH. The chemical approach to the control of tuberculosis. Science 1952;116(3006):129–34.
[31] Fox HH, Gibas JT. Synthetic tuberculostats. IV. Pyridine carboxylic acid hydrazides and benzoic acid hydrazides. J Org Chem 1952;17:1653–60.
[32] Fox HH, Gibas JT. Synthetic tuberculostats. VII. Monoalkyl derivatives of isonicotinylhydrazine. J Org Chem 1953;18:994–1002.
[33] Donald J, Abraham MM, editors. Burger's medicinal chemistry, drug discovery and development. 8 ed., 7. Wiley-Interscience; 2021.
[34] Kato T, Yamanaka H, Hamaguchi F. Studies on ketene and its derivatives. Iv. Reactions of diketene with isonicotinic acid hydrazide. Yakugaku Zasshi: J Pharm Soc Jpn 1963;83:741.
[35] Pretsch E, et al. Structure determination of organic compounds. Berlin: Springer-Verlag; 2000.
[36] Saha A, et al. Development and assessment of green synthesis of hydrazides. 2010.
[37] National Institute of Advanced Industrial Science and Technology (Japan). AIST: integrated spectral database system of organic compounds. 2011.
[38] Somani RR, Shirodkar P. Synthesis, antibacterial and antitubercular evaluation of some 1, 3, 4-oxadiazole analogues. Asian J Chem 2008;20(8):6189.
[39] Aziz DB, et al. Rifabutin is active against *Mycobacterium abscessus* complex. AAC (Antimicrob Agents Chemother) 2017;61(6). e00155-17.
[40] Weinstein MP, Lewis JS. The clinical and laboratory standards institute subcommittee on antimicrobial susceptibility testing: background, organization, functions, and processes. J Clin Microbiol 2020;58(3).
[41] Lakshminarayana SB, et al. Comprehensive physicochemical, pharmacokinetic and activity profiling of anti-TB agents. J Antimicrob Chemother 2015;70(3):857–67.
[42] Clinical, Institute LS. Performance standards for antimicrobial susceptibility testing. PA: Clinical and Laboratory Standards Institute Wayne; 2017.
[43] El-Fahm A, Abdul-Ghani M. TFFH as a useful reagent for the conversion of carboxylic acids to anilides, hydrazides and azides. Org Prep Proced Int 2003;35(4):369–74.
[44] Dydio P, Zielinski T, Jurczak J. Bishydrazide derivatives of isoindoline as simple anion receptors. J Org Chem 2009;74(4):1525–30.
[45] Gagneux S, et al. Variable host-pathogen compatibility in *Mycobacterium tuberculosis*. Proc Natl Acad Sci U S A 2006;103(8):2869–73.
[46] Senghore M, et al. Evolution of *Mycobacterium tuberculosis* complex lineages and their role in an emerging threat of multidrug resistant tuberculosis in Bamako, Mali. Sci Rep 2020;10(1):327.
[47] Wu M-L, et al. NTM drug discovery: status, gaps and the way forward. Drug Discov Today 2018;23(8):1502–19.
[48] Zeller EA, et al. Experientia 1952;8:349.
[49] Zeller EA, Barsky J. In vivo inhibition of liver and brain monoamine oxidase by 1-Isonicotinyl-2-isopropyl hydrazine. Proc. Soc. Exp. Biol. Med. 1952;81(2):459–61.
[50] Seydel JK, et al. Mode of action and quantitative structure-activity correlations of tuberculostatic drugs of the isonicotinic acid hydrazide type. J Med Chem 1976;19(4):483–92.
[51] Schaper KJ, Seydel JK. Structure-activity correlations in a homologous series of 2-substituted isonicotinic acid hydrazides. In: Tichý M, editor. Quantitative structure-activity relationships: proceedings of the conference on chemical structure—biological activity relationships: quantitative approaches prague, czechoslovakia 27 to 29 june, 1973. Basel: Birkhäuser Basel; 1976. p. 119–24.
[52] Laborde J, et al. Synthesis, oxidation potential and anti–mycobacterial activity of isoniazid and analogues: insights into the molecular isoniazid activation mechanism. Chemistry 2016;1(2):172–9.
[53] Laborde J, Deraeve C, Bernardes-Génisson V. Update of antitubercular prodrugs from a molecular perspective: mechanisms of action, bioactivation pathways, and associated resistance. ChemMedChem 2017;12(20):1657–76.
[54] Zhao X, Yu S, Magliozzo RS. Characterization of the binding of isoniazid and analogues to *Mycobacterium tuberculosis* catalase-peroxidase. Biochemistry 2007;46(11):3161–70.
[55] Rawat R, Whitty A, Tonge PJ. The isoniazid-NAD adduct is a slow, tight-binding inhibitor of InhA, the *Mycobacterium tuberculosis* enoyl reductase: adduct affinity and drug resistance. Proc Natl Acad Sci. 2003;100(24):13881.
[56] Wiseman B, et al. Isonicotinic acid hydrazide conversion to Isonicotinyl-NAD by catalase-peroxidases. J Biol Chem 2010;285(34):26662–73.
[57] Hartkoorn RC, et al. Towards a new tuberculosis drug: pyridomycin - nature's isoniazid. EMBO Mol Med 2012;4(10):1032–42.